Applied Surface Science 255 (2009) 6745–6749

Contents lists available at ScienceDirect

Applied Surface Science

journal homepage: www.elsevier.com/locate/apsusc

Annealing temperature dependent electrical and optical properties of ZnO and MgZnO films in hydrogen ambient

Weiwei Liu [a,b], Bin Yao [a,*], Yongfeng Li [a,b], Binghui Li [a], Changji Zheng [a,b], Bingye Zhang [a,b], Chongxin Shan [a], Zhenzhong Zhang [a], Jiying Zhang [a], Dezhen Shen [a]

[a] Laboratory of Excited State Processes, Changchun Institute of Optics, Fine Mechanics and Physics, Chinese Academy of Sciences, Changchun 130021, People's Republic of China
[b] Graduate School of the Chinese Academy of Sciences, Beijing 100049, People's Republic of China

ARTICLE INFO

Article history:
Received 1 January 2009
Received in revised form 25 February 2009
Accepted 1 March 2009
Available online 11 March 2009

Keywords:
Thin films
Annealing
Electrical properties
Optical properties

ABSTRACT

Un-doped ZnO and MgZnO thin films were deposited on *c*-plane sapphire substrates by molecular-beam epitaxy (MBE) and subsequently annealed in hydrogen ambient at 200–500 °C with a step of 100 °C. Hall-effect measurements show that annealing temperature has great effect on the electrical property of both ZnO and MgZnO films. The electron concentration of both ZnO and MgZnO films increases with annealing temperature ranging from 200 °C to 400 °C, and then decreases, which is attributed to incorporation of H into ZnO as a shallower donor during the annealing process and change of solid solubility of hydrogen in ZnO and MgZnO films with annealing temperature. The D^0X emission is related to the hydrogen in MgZnO film and the donor level of the H is estimated to be 33.5 meV. It is also found that the controversial luminescence band at 3.310 eV can be formed in un-doped ZnO film upon annealing and its intensity increases with increasing annealing temperature, implying that this band may be not related to p-type doping.

1. Introduction

Attribute to its wide direct band gap of 3.37 eV and high exciton binding energy (60 meV), ZnO has received much attention for its potential applications in blue and ultraviolet (UV) light emitting diodes (LED), laser diodes, piezoelectric, ferroelectric, solar, surface acoustic wave devices and field effect transistors. ZnO now can be grown using a variety of epitaxial techniques and high quality bulk single crystal wafers are available [1–4].

As-grown un-doped ZnO always show n-type conductivity, but the origin of the n-type conductivity is still controversial. However, a recent first-principle investigation shows that because of large formation energy, none of the native defects can offer so high-concentration shallow donor [5]. Therefore, the origin of n-type conductivity is not attributed to native defects. Based on the theory and experiments, hydrogen can be incorporated into high concentrations and behaves as a shallow donor but not amphoteric in ZnO [6,7]. Many researchers believe that interstitial hydrogen as a shallow donor is one possibility for the prevalence conductivity.

At present, there have been many investigations on the effects of hydrogen on ZnO in several ways, including the modification of the electrical and optical properties of ZnO [8–15]. Van de Walle has shown that the bond center of the Zn–O bond is the most stable position for interstitial hydrogen (H_i) [6]. In particular, the activation energy of hydrogen in ZnO was about 35 ± 5 meV has been reported [16]. Meanwhile, many methods have been applied to obtain ZnO materials doped with hydrogen, such as direct or remote H_2 plasma irradiation [9,10,13,14], H_2 ion implantation [7,8,11,12], add H_2 to the reaction gas during film deposition [15], H_2 annealing [17], etc. There have been some reports about the incorporation and out-diffusion of hydrogen in single-crystal ZnO doped with hydrogen by ion-implantation or hydrogen plasma exposure [9,18,19]. These results have shown that hydrogen exhibits a very rapid diffusion in ZnO film and subsequent annealing at 600–700 °C is sufficient to evolve hydrogen out of the ZnO film. The incorporation depth of the hydrogen in ZnO film can be reached at 25 mm when exposure to hydrogen plasmas at moderate temperature. The electrical conductivity of ZnO film can be increased after annealing in hydrogen ambient at some temperatures and the increment of the electrical conductivity varied with the dopant in as-grown ZnO films [20]. Besides annealing time [21], annealing temperature is considered as one of the sensitive factors for effecting the crystal quality, oxygen defect and local structure of semiconductor oxides during annealing process. However, there is no systematic investigation on the

* Corresponding author at: No. 16, Dong Nanhu Road, Changchun 130033, PR China. Tel.: +86 431 86176355; fax: +86 431 85682964.
E-mail address: yaobin196226@yahoo.com.cn (B. Yao).

0169-4332/$ – see front matter © 2009 Elsevier B.V. All rights reserved.
doi:10.1016/j.apsusc.2009.03.001

properties of the ZnO films annealed in hydrogen ambient at different temperatures.

In this work, annealing process carried out in hydrogen ambient was used to introduce hydrogen into ZnO and MgZnO films. The properties of the ZnO and MgZnO thin films annealed in hydrogen were studied as a function of the annealing temperature.

2. Experiment details

The growth of un-doped ZnO and MgZnO films were carried out using a V80H molecular-beam epitaxy (MBE) system equipped with Knudsen-cells for a Zn solid source (99.999%) and an Mg solid source (99.9999%), and O_2 (99.99%) was used as O source activated by an Oxford Applied Research Model HD25 rf (13.56 MHz) atomic source. The *c*-plane sapphire was used as substrate. The detail growth process can be seen elsewhere [22]. The as-grown ZnO and MgZnO films thickness are about 900 nm and 500 nm, respectively. The as-grown ZnO and MgZnO films were cut into small pieces, and they subsequently annealed in high-purity hydrogen (99.999%) for 1 h at 200–500 °C with a step of 100 °C. The annealing process was carried out at atmosphere pressure using the system of metal–organic chemical vapor deposition (MOCVD). After annealing, all of the samples were cooled at a rate of 10 °C/min down to room temperature in hydrogen ambient, and then taken out for characterization.

Structures of the films were characterized by X-ray diffraction (XRD) using a D/max-RA X-ray diffractometer with Cu Kα radiation, and all diffraction peaks were calibrated by Al_2O_3 (0 0 6) peak at 41.68°. The absorption spectra of the ZnO and MgZnO films were recorded by UV–vis near infrared spectrophotometer. Photoluminescence measurement was performed by the excitation from a 325-nm He–Cd laser with 50 mW power. The electrical properties of the samples were measured in Van der Pauw configuration by a Hall analyzer (Lakeshore7707) at room temperature. Hall measurement was carried out under five different magnetic field (3, 6, 9, 12, and 15 kG). The relevant inaccuracy of the electrical data is about 2%. A hatachi S4800 energy dispersive spectroscopy (EDS) was used to determine the Mg content in MgZnO film, and the acceleration voltage and the magnification of EDS were 10 kV and 5000, respectively.

3. Results and discussion

Fig. 1 shows the absorption spectra of the as-deposited ZnO and MgZnO films taken at room temperature. Both of the films exhibited sharp absorption edges, implying that the as-grown films have high crystalline quality. This result is consistent with the result of XRD, as illustrated in the inset in Fig. 1, both of them show a highly intense (0 0 2) diffraction peak with narrow full-width at half-maximum. The shift in absorption edge of the MgZnO film towards to the higher energy side indicates that Mg incorporated into ZnO film, in good agreement with the result reported by Ohtomo [23]. By fitting $(\alpha h\nu)^2$ vs. $h\nu$ plot shown in Fig. 1 with the relationship of $(\alpha h\nu)^2 \propto (h\nu - E_g)$ (where α is the absorption coefficient, $h\nu$ is the photon energy and E_g is optical band gap), the E_g is estimated to be 3.421 eV for the MgZnO film and 3.294 eV for the ZnO film. The Mg content in the MgZnO layer was determined to be 4 at.% by using EDS measurement.

Fig. 2 shows the XRD patterns of ZnO samples before and after annealing. Before annealing, the pattern shows a strong (0 0 2) diffraction peak. After annealing, obviously, the (0 0 2) peak consists of two peaks, the strong one comes from diffraction of $CuK_{\alpha 1}$ radiation and the weak one comes from diffraction of $CuK_{\alpha 1}$ radiation. This suggests that annealing treatment improves the crystalline quality of the films. It is worth noticing that the diffraction angle of (0 0 2) peak of the ZnO decreases with

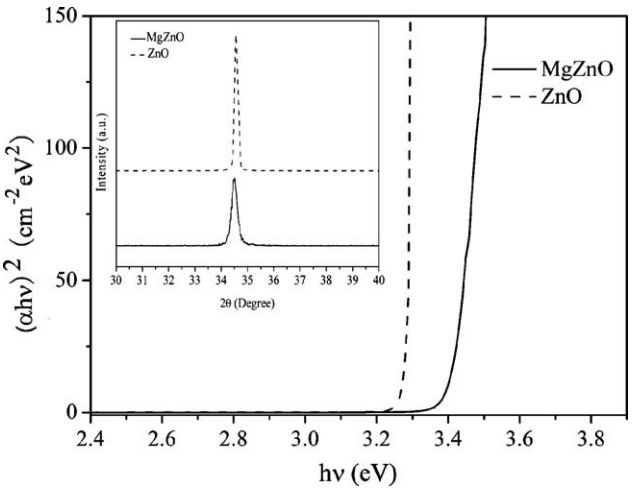

Fig. 1. The absorption spectra of the as-grown ZnO film (dashed line) film and MgZnO (solid line) film taken at room temperature. The inset shows the XRD of both films.

increasing annealing temperature. It has been reported that ZnO (0 0 0 1) grows with a 30° in-plane rotation relative to *c*-Al_2O_3 (0 0 0 1) substrate and ZnO layer suffer a compressive stress in the plane of the film due to lattice misfit [24]. However, a recent investigation show that the strain in ZnO layers grown on *c*-Al_2O_3 substrates is dependent on the thickness of the ZnO layers [25]. ZnO films experience compressive strain in-plane attributed to lattice misfit for thickness below 200 nm and tensile strain in-plane attributed to thermal stress above 200 nm. Since the ZnO films used in our experiment have a thickness about 900 nm, ZnO films suffer a tensile strain in-plane and compressive stress in *c*-axis direction attributed to thermal stress. The gradual decrease of the 2θ with increasing annealing temperature suggests that the compressive stress in *c*-axis direction is partly relaxed.

Tables 1 and 2 illustrate room temperature electrical properties of MgZnO and ZnO films after annealing in hydrogen ambient at different temperature as well as as-grown samples, respectively. The electron concentration in as-grown MgZnO film is two orders of magnitude lower than that of in as-grown ZnO film. It is well known that the formation energy of Zinc vacancy (V_{Zn}) can be decreased when Mg was incorporated into ZnO, indicating that V_{Zn} is easier to form in $Mg_xZn_{1-x}O$ films [26]. Moreover, the acceptor-like defects (i.e., interstitial oxygen O_i and Zn vacancy V_{Zn}) could compensate the n-type doping effect of Zn_i or/and V_o, which leads

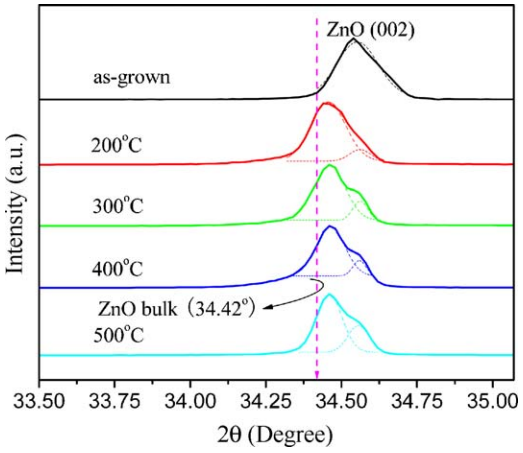

Fig. 2. The X-ray diffraction patterns of ZnO thin films before and after annealing in hydrogen ambient at different temperatures.

Table 1
Room temperature electrical properties of MgZnO films after annealing in hydrogen ambient at different temperature and vacuum at 400 °C as well as as-grown sample.

Annealing ambient and temperature	ρ (Ω cm)	n (cm^{-3})	μ ($cm^2/(V\,s)$)
MgZnO (as-grown)	121.52	7.14E+16	1.24
MgZnO (H_2/200 °C)	36.06	1.22E+17	2.57
MgZnO (H_2/300 °C)	0.55	2.63E+18	4.16
MgZnO (H_2/400 °C)	0.25	5.37E+18	4.71
MgZnO (H_2/500 °C)	1.02	1.94E+18	3.35
MgZnO (vacuum/400 °C)	5.23	1.08E+18	1.15

Table 2
Room temperature electrical properties of ZnO films after annealing in hydrogen ambient at different temperature and vacuum at 400 °C as well as as-grown sample.

Annealing ambient and temperature	ρ (Ω cm)	n (cm^{-3})	μ ($cm^2/(V\,s)$)
ZnO (as-grown)	0.05	3.72E+18	35.34
ZnO (H_2/200 °C)	0.04	5.40E+18	28.05
ZnO (H_2/300 °C)	0.03	6.54E+18	28.11
ZnO (H_2/400 °C)	0.02	1.34E+19	28.92
ZnO (H_2/500 °C)	0.02	6.52E+18	44.65
ZnO (vacuum/400 °C)	0.04	3.68E+18	47.57

to lower the electron concentration in MgZnO film. In addition, the introduction of Mg can move up the conduction band edge and increase the band gap, thus lower the n-type background.

From Tables 1 and 2, it can be concluded that annealing temperature play an important role on the electrical property of MgZnO and ZnO films. The electron concentration of both ZnO and MgZnO films increases with annealing temperature ranging from 200 °C to 400 °C, thereafter decreases. The electron concentration of the MgZnO annealed in hydrogen ambient at 400 °C is two orders of magnitude larger than that of the as-grown MgZnO film. As for ZnO film, the electron concentration of the ZnO annealed in hydrogen ambient at 400 °C is one order of magnitude larger than that of the as-grown ZnO film. Increasing in electron concentration was attributed to Zn_i generated during annealing process [17], but as mentioned in introduction, none of the native defects can offer so high-concentration shallow donor. Furthermore, it is difficult to explain the decreasing in electron concentration after annealing at 500 °C. But, it is worth noticing that the changes in the electron concentration are similar to the changes in the solid solubility of hydrogen in ZnO film. It was reported that hydrogen can be incorporated into bulk, single-crystal ZnO during exposure to hydrogen plasmas at moderate temperature and acts as a shallow donor. Subsequent annealing at 500–600 °C in nitrogen is sufficient to drive hydrogen out from ZnO [9]. Therefore, the increase in electron concentration in the temperature range from 200 °C to 400 °C, as shown in Tables 1 and 2, can be reasonably attributed to that hydrogen diffuses into ZnO and MgZnO films and forms a shallow donor during annealing in hydrogen ambient.

In order to further confirm this conclusion, MgZnO and ZnO films have been annealed in vacuum for 1 h at 400 °C. The carrier concentration and electrical resistivity of the MgZnO and ZnO films annealed in vacuum at 400 °C are also shown in Tables 1 and 2, respectively. It is found that the electron concentration of MgZnO and ZnO films annealed in hydrogen ambient is five and four times larger than of the MgZnO and ZnO films annealed in vacuum at 400 °C, respectively. This result is further support the argument that increasing in electron concentration is attributed to the hydrogen diffuses into MgZnO and ZnO films and forms a shallow donor during annealing in hydrogen ambient.

The typical PL spectra of as-grown and annealed MgZnO films measured at 80 K are shown in Fig. 3. The PL spectrum of as-deposited MgZnO is dominated by two peaks centre at 3.447 eV (labeled as A) and 3.406 eV (labeled as B). According to their energy

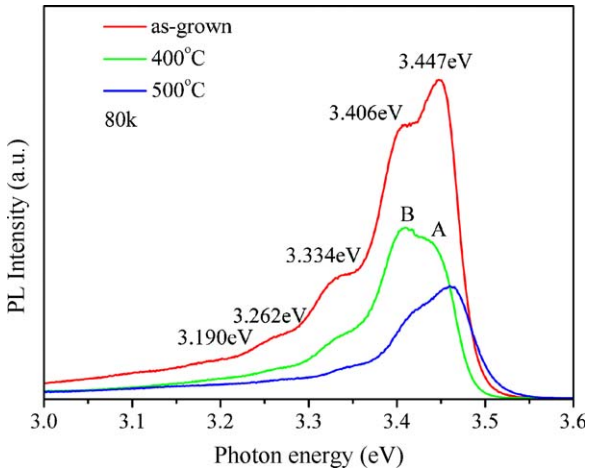

Fig. 3. Typical PL spectra of MgZnO films before and after annealing in hydrogen ambient at different temperatures measured at 80 K.

values, the emission peaks at 3.334 eV, 3.262 eV and 3.190 eV are assigned to three longitudinal optical phonon replicas of the emission band B. It is interesting to note that change in the intensity ratio of emission band B to emission band A agrees well with the evolution of the electron concentration of annealed samples. The intensity ratio of emission band B to emission band A enhances with the increasing electron concentration. This could be explained by the number of electrons produced by hydrogen. It can be indicated that an increase in the number of H, which can be donors, seems to be one origin of the higher electron concentration of MgZnO and ZnO films. Therefore, the origin of emission band B at 3.406 eV is suggested to be related to neutral donor bound exciton (D^0X), while the emission band A at 3.447 eV could be suggested as free exciton (FX) emission. Above results suggest that annealing temperature can greatly affect the photoluminescence spectra of MgZnO films.

The temperature dependent PL spectra of the MgZnO film annealed at 400 °C was also measured (not shown here). The PL intensity of the donor-bound exciton (D^0X) decreases gradually with increasing temperature, as shown in Fig. 4. The integral PL intensity usually decreases with temperature due to the thermal quenching as [27]

$$I(T) = \frac{I(0)}{1 + A\exp[-(E_a/k_B T)]} \quad (1)$$

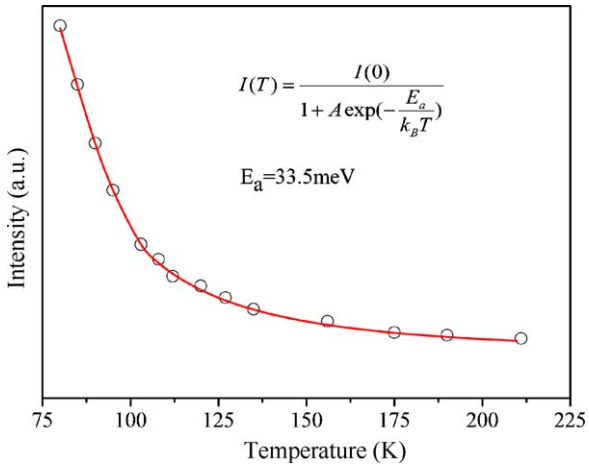

Fig. 4. The integrated intensity of D^0X as a function of measure temperature and the fitting curve using Eq. (1).

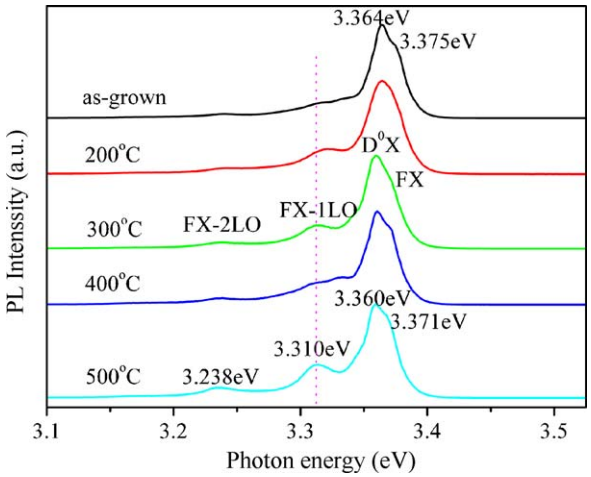

Fig. 5. Typical PL spectra of ZnO films before and after annealing in hydrogen ambient at different temperatures measured at 80 K.

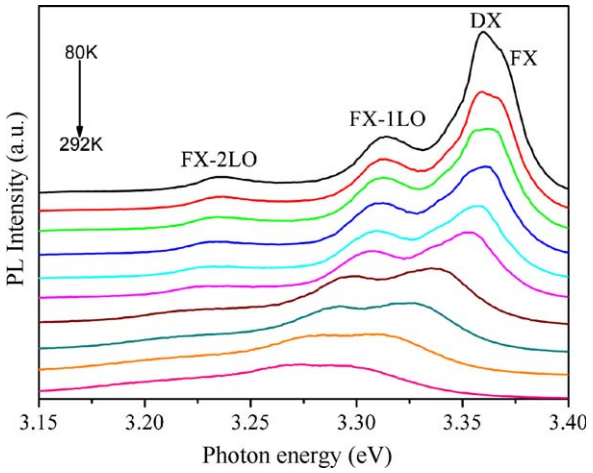

Fig. 6. Temperature dependence of the PL spectra of the ZnO annealed at 500 °C in hydrogen ambient. The spectra are shifted in the vertical direction for clarity.

where A is a parameter, $I(0)$ is the intensity of the peak emission at a temperature of 0 K, E_a is the activation energy in the thermal quenching process, and k_B is the Boltzmann constant. The curve in Fig. 4 represents the results of the best fit according to Eq. (1). The fitting value of E_a is equal to 33.5 meV, which is close to the activation energy of hydrogen in ZnO (=35 ± 5 meV) [16]. According to above consideration, it is reasonable to suggest that hydrogen can be incorporated into MgZnO films by the annealing process and increase the electron concentration of the annealed films, and furthermore, the donor states causing the D^0X emission are related to the hydrogen in MgZnO film.

Fig. 5 shows the typical PL spectra of as-grown and annealed ZnO films measured at 80 K. As-deposited ZnO shows the UV emission lines located at 3.375 eV and 3.364 eV, which are attributed to a free exciton and a neutral donor bound exciton, respectively. After annealing in the entire rang of annealing temperatures, all of the UV emission lines show a red shift by the relaxation of built-in strain in ZnO, which is consistent with the result of XRD shown in Fig. 2. Furthermore, the peaks at 3.310 eV and 3.238 eV also appeared. In previous reports, the emission near 3.310 eV was attributed to different recombination processes, such as neutral acceptor bond exciton (A^0X), donor-acceptor pair (DAP), electron transition from conduct band to an acceptor level (FA), and first LO replica of the FX [28–31]. In fact, the origin of this emission band is still not clear up to now.

In the present work, we suggest that the emission band located at 3.310 eV formed during the annealing process is the first LO photon replica of the FX recombination. Fig. 6 shows the temperature dependence of the edge emission region for the ZnO film annealed at 500 °C. The 3.371 eV peak is assigned to the free exciton recombination. As the temperature is increasing, the FX becomes stronger in intensity relative to the D^0X peaks and finally becomes the dominant. These phenomena are attributed to the decomposition of bound exciton to free exciton by thermal energy at a high temperature. The intensity of the peak at 3.310 eV changes with the change in the intensity of FX, indicating that the 3.310 eV emission band is related to the FX recombination. From Ref. [32], we can concluded that the energy separation between the free-exciton emission (FX) and its first LO photon replica exhibit a strong temperature dependence. The temperature dependence of the energy separation at low temperature (<80 K) can be expressed as [33]

$$\Delta E = \hbar\omega_{LO} - \tfrac{3}{2}k_B T \quad (2)$$

where k_B is the Boltzmann constant and $\hbar\omega_{LO}$ is the LO-phonon energy of ZnO. Using Eq. (2), the calculated value of the energy separation between the free-exciton emission (FX) and its first LO photon replica was about 62 meV at 80 K, which is close to the 61 meV separated energy between 3.310 eV and FX obtained from the PL spectra shown in Fig. 6. Therefore strongly support the argument that the 3.310 eV peak comes from the first LO photon replica of the FX recombination and not related to p-type doping. The intensity of the emission band at 3.310 eV increases with increasing annealing temperature, indicating that the crystalline quality of ZnO films were gradually improved upon annealing which is consistent with the result of XRD. The second LO photon replica located at 3.238 eV can also be seen in Fig. 6.

4. Conclusions

Temperature-controlled annealing process on ZnO and MgZnO films in hydrogen ambient was introduced in this study for the purpose of modulating the electrical and optical properties of the films deposited on *c*-plane sapphire substrates by molecular-beam epitaxy (MBE). Not only hydrogen but also annealing temperature was playing an important role in the changes of the electrical and optical properties of the ZnO and MgZnO films. The crystalline quality of the films can be gradually improved upon annealing. The electron concentration of both ZnO and MgZnO films increases with annealing temperature ranging from 200 °C to 400 °C, thereafter decreases. The changes of the electron concentration upon the annealing temperature were attributed to the effect of annealing temperature on the solid solubility of hydrogen in ZnO and MgZnO films. For MgZnO films, the change in the intensity ratio of neutral donor bound exciton (D^0X) emission to free exciton (FX) emission is the same as the evolution of the electron concentration of the annealed samples. The donor states causing the D^0X emission are related to the hydrogen in MgZnO film and the donor level of the H is estimated to be 33.5 meV. For ZnO films, the controversial luminescence band located at 3.310 eV formed upon annealing is ascribed to the first LO replica of the FX recombination. It is, therefore, the 3.31 eV emission band may be not related to the p-type doping.

Acknowledgements

This work is supported by the Key Project of National Natural Science Foundation of China under Grant no. 50532050, the "973" program under Grant no. 2006CB604906, the Innovation Project of

Chinese Academy of Sciences, the National Natural Science Foundation of China under Grant nos. 6077601, 60506014, 10674133, 60806002 and 10874178.

References

[1] Z.K. Tang, G.K.L. Wong, P. Yu, Appl. Phys. Lett. 72 (1998) 3270.
[2] D.C. Look, Mater. Sci. Eng. 80 (2001) 383.
[3] K. Iwata, P. Fons, A. Yamada, K. Matsubara, S. Niki, J. Cryst. Growth 209 (2000) 526.
[4] Y.W. Heo, V. Varadarajan, M. Kaufman, K. Kim, D.P. Nortona, Appl. Phys. Lett. 81 (2002) 3046.
[5] A.F. Kohan, G. Ceder, D. Morgan, C.G. Van de Walle, Phys. Rev. B. 61 (2000) 15019.
[6] C.G. Van de Walle, Phys. Rev. Lett. 85 (2000) 1012.
[7] E.V. Monakhov, A.Y. Kuznetsov, J.S. Christensen, K. Maknys, B.G. Svensson, Superlattices Microstruct. 38 (2005) 472–478.
[8] S. Kohiki, I. Nishitani, T. Wada, T. Hirao, Appl. Phys. Lett. 64 (1994) 2876.
[9] K. Ip, M.E. Overberg, Y.W. Heo, D.P. Norton, S.J. Pearton, Solid-State Electron. 47 (2003) 2255.
[10] A.Y. Polyakov, N.B. Smirnov, A.V. Govorkov, K. Ip, M.E. Overberg, Y.W. Heo, D.P. Norton, S.J. Pearton, B. Luo, F. Ren, J.M. Zavada, J. Appl. Phys. 94 (2003) 400.
[11] J.-K. Lee, M. Nastasi, D.W. Hamby, D.A. Lucca, Appl. Phys. Lett. 86 (2005) 171102.
[12] Z. Zhou, K. Kato, T. Komaki, M. Yoshino, H. Yukawa, M. Morinaga, K. Morita, J. Eur. Ceram. Soc. 24 (2004) 139.
[13] N. Ohashi, T. Ishigaki, N. Okada, T. Sekiguchi, I. Sakaguchi, H. Haneda, Appl. Phys. Lett. 80 (2002) 2869.
[14] B. Theys, V. Sallet, F. Jomard, A. Lusson, J.-F. Rommeluère, Z. Teukam, J. Appl. Phys. 91 (2002) 3922.
[15] W.F. Liu, G.T. Du, Y.F. Sun, J.M. Bian, Y. Cheng, T.P. Yang, Y.C. Chang, Y.B. Xu, Appl. Surf. Sci. 253 (2007) 2999–3003.
[16] D.M. Hofmann, A. Hofstaetter, F. Leiter, H. Zhou, F. Henecker, B.K. Meyer, S.B. Orlinskii, J. Schmidt, P.G. Baranov, Phys. Rev. Lett. 88 (2002) 045504.
[17] Y. Natsume, H. Sakata, J. Mater. Sci.: Mater. Electron. 12 (2001) 87–92.
[18] K. Ip, M.E. Overberg, Y.W. Heo, D.P. Norton, S.J. Pearton, S.O. Kucheyev, C. Jagadish, J.S. Williams, R.G. Wilson, J.M. Zavada, Appl. Phys. Lett. 81 (2002) 3996.
[19] K. Ip, M.E. Overberg, Y.W. Heo, D.P. Norton, S.J. Pearton, C.E. Stutz, B. Luo, F. Ren, D.C. Look, J.M. Zavada, Appl. Phys. Lett. 82 (2003) 385.
[20] Z. Zhou, K. Kato, T. Komaki, M. Yoshino, H. Yukawa, M. Morinaga, Int. J. Hydrogen Energy 29 (2004) 323–327.
[21] B.-Y. Oh, M.-C. Jeong, D.-S. Kim, W. Lee, J.-M. Myoung, J. Cryst. Growth 281 (2005) 475–480.
[22] Y.M. Lu, C.X. Wu, Z.P. Wei, Z.Z. Zhang, D.X. Zhao, J.Y. Zhang, Y.C. Liu, D.Z. Shen, X.W. Fan, J. Cryst. Growth 278 (2005) 299–304.
[23] A. Ohtomo, M. Kawasaki, T. Koida, K. Masubuchi, H. Koinuma, Y. Sakurai, Y. Yoshida, T. Yasuda, Y. Segawa, Appl. Phys. Lett. 72 (1998) 2466.
[24] Ü. Özgür, Y.I. Alivov, C. Liu, A. Teke, M.A. Reshchikov, S. Doğan, V. Avrutin, S.-J. Cho, H. Morkoç, J. Appl. Phys. 98 (2005) 041301.
[25] S.H. Park, T. Hanada, D.C. Oh, T. Minegishi, H. Goto, G. Fujimoto, J.S. Park, I.H. Im, J.H. Chang, M.W. Cho, T. Yao, Appl. Phys. Lett. 91 (2007) 231904.
[26] Y.F. Li, B. Yao, Y.M. Lu, Y.Q. Gai, C.J. Zheng, Z.Z. Zhang, B.H. Li, D.Z. Shen, X.W. Fan, Z.K. Tang, Appl. Phys. Lett. 91 (2007) 232115.
[27] D.S. Jiang, H. Jung, K. Ploog, J. Appl. Phys. 64 (1988) 1371.
[28] D.C. Look, D.C. Reynolds, C.W. Litton, R.L. Jones, D.B. Eason, G. Cantwell, Appl. Phys. Lett. 81 (2002) 1830.
[29] J.F. Rommeluère, L. Svob, F. Jomard, J. Mimila-Arroyo, A. Lusson, V. Sallet, Y. Marfaing, Appl. Phys. Lett. 83 (2003) 287.
[30] J.W. Sun, Y.M. Lu, Y.C. Liu, D.Z. Shen, Z.Z. Zhang, B.H. Li, J.Y. Zhang, B. Yao, D.X. Zhao, X.W. Fan, J. Appl. Phys. 102 (2007) 043522.
[31] H.J. Ko, Y.F. Chen, T. Yao, K. Miyajima, A. Yamamoto, T. Goto, Appl. Phys. Lett. 72 (1998) 2466.
[32] A. Teke, Ü. Özgür, S. Doğan, X. Gu, H. Morkoç, B. Nemeth, J. Nause, H.O. Everitt, Phys. Rev. B. 70 (2004) 195207.
[33] L. Wang, N.C. Giles, J. Appl. Phys. 94 (2003) 973.